CHEMICAL ENGINEERING TRANSACTIONS
VOL. 57, 2017
A publication of AIDIC
The Italian Association of Chemical Engineering
Online at www.aidic.it/cet
Guest Editors: Sauro Pierucci, Jiří Jaromír Klemeš, Laura Piazza, Serafim Bakalis
Copyright © 2017, AIDIC Servizi S.r.l.
ISBN 978-88-95608- 48-8; **ISSN** 2283-9216
DOI: 10.3303/CET1757151

Hydrogen Production by Reforming of Methane over $NiAl_2O_4/Ce_xZr_{1-x}O_2$ Catalysts

Miryam Gil-Calvo, Cristina Jiménez-González, Beatriz de Rivas, Jose-Ignacio Gutiérrez-Ortiz, Ruben López-Fonseca*

Department of Chemical Engineering, Faculty of Science and Technology, University of The Basque Country UPV/EHU, P.O. Box 644, E-48080 Bilbao, Spain.
ruben.lopez@ehu.eus

This work was focused on the study of the catalytic behaviour of nickel aluminate supported either on ceria or ceria-zirconia ($NiAl_2O_4/Ce_xZr_{1-x}O_2$, x= 0.13 and 1, 14 wt.% Ni) for the steam reforming and partial oxidation of methane. Activity results revealed that these catalytic formulations showed a notable performance for POM under stoichiometric conditions (molar ratio O/C = 1), irrespective of the composition of the support. However, under more severe reforming conditions (O/C = 0.8) $NiAl_2O_4/CeO_2$ was the optimal catalyst as its marked reducibility helped in minimising the negative effect of coking. Conversely, the $NiAl_2O_4/Ce_{0.13}Zr_{0.87}O_2$ sample was the most efficient system for SRM due to its high hydrothermal stability.

1. Introduction

Methane reforming represents an attractive strategy for hydrogen production in the near/mid-term owing to its abundance, high H/C molar ratio and already available distribution network. As an alternative to expensive noble metal (Rh) catalysts the use of cheaper nickel catalysts with loadings between 5-20 wt.% is preferred. In this sense, nickel aluminate ($NiAl_2O_4$) can be considered an interesting alternative to the conventional NiO as Ni-based catalyst precursor since it provides highly dispersed metallic nickel crystallites on alumina after an appropriate reduction carried out at temperatures above 825 ºC (Boukha et al., 2016). However, nickel aluminate system remains vulnerable to coking at the high temperatures required in the reforming process. In order to mitigate this negative effect, a possible solution would be to support the spinel on reducible oxides such as CeO_2 and $Ce_xZr_{1-x}O_2$. In fact, it is expected that their redox properties, high oxygen storage capacity and metal-ceria strong interactions would attenuate the deactivation by keeping the active metal sites free of carbon species (Roh et al., 2002). Hence, the combination of the highly dispersed active phase provided by nickel aluminate and the high oxygen mobility given by ceria-based supports could result in the ideal features for reforming applications. On the basis of this background, in this work the innovative $NiAl_2O_4/Ce_xZr_{1-x}O_2$ catalytic formulation was experimentally examined for both partial oxidation (POM) and steam reforming of methane (SRM).

2. Experimental

The support materials used in this study were CeO_2 (28 $m^2\ g^{-1}$, Rhodia) and $Ce_{0.13}Zr_{0.87}O_2$, CZ, (24 $m^2\ g^{-1}$, Mel Chemicals) which were previously calcined at 850 ºC for 8 h. The catalysts, were synthesised by precipitation at pH = 8 from nickel acetate and aluminum nitrate and the nominal Ni loading was fixed at 14 wt.% for both samples. Finally, after drying at 110 ºC the samples were calcined at 850 ºC for 4 h. This last step led to the formation of the nickel aluminate. The resultant catalysts were denoted as $NiAl\text{-}CeO_2$ and NiAl-CZ. As reference catalysts, a bulk $NiAl_2O_4$ (NiAl) and a commercial Rh/Al_2O_3 sample (1 %Rh/Al_2O_3, 132 $m^2\ g^{-1}$, Alfa Aesar) were employed. The catalysts were thoroughly characterised by ICP-AES, N_2 physisorption, XRD, XPS, H_2-TPR, TEM, TGA-MS and Raman spectroscopy. Catalytic tests were performed uploading 125 mg of catalyst in a bench-scale fixed-bed reactor at atmospheric pressure and with an inlet flow rate of 0.8 L min^{-1}.

Please cite this article as: Gil-Calvo M., Jimenez-Gonzalez C., De Rivas B., Gutierrez-Ortiz J.I., Lopez-Fonseca R., 2017, Hydrogen production by reforming of methane over nial2o4/cexzr1-xo2 catalysts, Chemical Engineering Transactions, 57, 901-906 DOI: 10.3303/CET1757151

Prior to reaction, the nickel catalysts were activated in situ by reduction with 5 vol.%H_2/N_2 at 850 ºC for 2 h. Depending on the reforming process, the following reaction conditions were adopted:

For SRM: i) 10 vol.%CH_4, 6-40 vol.%H_2O and 50-84 vol.%N_2 (volume hourly space velocity (VHSV)=38.4 L CH_4 g^{-1} h^{-1}; H_2O/C=0.6-4; 200-850 ºC; 9 h)

For POM: i) 10 vol. %CH_4, 5 vol.%O_2 and 85 vol.%N_2 (VHSV = 38.4 L CH_4 g^{-1} h^{-1}; O/C=1; 700 ºC; 3 h)
ii) 15.6 vol.%CH_4, 6.3 vol.%O_2 and 78.1 vol.%N_2 (VHSV = 60 L CH_4 g^{-1} h^{-1}; O/C=0.8; 700 ºC; 30 h).

3. Results and discussion

3.1 Characterisation of the samples

The structural properties of the calcined precursors were analysed by XRD using the JCPDS database as a reference. The reflections at 2θ=37.1º, 45.1º, 59.3º and 65.7º observed in the patterns of the supported NiAl samples were in good agreement with the face-centred cubic structure of stoichiometric nickel aluminate (Ni/Al=1/2, JCPDS 78-1601). Interestingly, the absence of characteristic NiO signals (2θ=43.3º and 62.9º) suggested that the nickel was completely incorporated in the spinelic structure. In the bulk NiAl sample the stoichiometric nickel aluminate was found to be exclusively formed as well. Therefore, it was confirmed that the employed synthesis procedure was adequate to prepare samples with $NiAl_2O_4$ as main phase. Evidently, the characteristic peaks of the employed ceria-based supports were also present in the diffractograms of both precursors. Hence, the pattern of the NiAl-CeO_2 sample included signals corresponding to the cubic structure of the ceria (JCPDS 89-8436) while in the case of NiAl-CZ reflections associated with the tetragonal structure of the ceria-zirconia mixed oxide with a low Ce/Zr molar ratio (JCPDS 88-2397) could be distinguished. The oxidation state and the chemical environment of the nickel present on the surface of the precursors were examined by X-ray photoelectron spectroscopy. For both supported NiAl catalysts, as well as for the bulk NiAl sample, the XPS curves of the Ni $2p_{3/2}$ region were composed of two contributions; the principal peak attributed to nickel species and its satellite. The apparent symmetry of these main photoemission peaks suggested the existence of a unique homogeneous phase. Moreover, they were centred close to the theoretical binding energy of the $NiAl_2O_4$ (856.0 eV with respect to 856.1 eV for NiAl-CeO_2, 856.4 eV for NiAl-CZ and 855.4 eV for NiAl) thereby pointing out that nickel aluminate was the predominant phase at the surface level.

XRD analysis of the reduced samples confirmed that the reduction process used for the activation of the catalysts prior to reaction tests (850 ºC/ 2 h/ 5%$H_2(N_2)$) was appropriate to attain the complete conversion of nickel aluminate-based precursor into Ni/Al_2O_3. In fact, the XRD patterns contained the two phases resulting from this transformation, namely, metallic nickel (Ni^0 JCPDS 89-7128, signals at 2θ=44.7º, 51.9º and 76.5º) and γ-alumina (JCPDS 79-1558), and obviously the corresponding support. It must be noted that the XRD spectrum of NiAl-CeO_2 also revealed the formation of $CeAlO_3$, as a consequence of the interaction between the support and the alumina generated due to the reduction step ($2CeO_2+Al_2O_3+H_2 \rightarrow 2CeAlO_3+H_2O$) (Luisetto et al., 2015). In contrast, the presence of this phase was not detected in NiAl-CZ, probably owing to the lower proportion of cerium of this support. Accordingly, the alumina signals at 2θ=46.7º and 66.6º were more pronounced in this catalyst.

The physical properties of the supports and the synthesised catalysts were measured by N_2 physisorption (Table 1). In accordance with the IUPAC classification all sorption isotherms were type IV, with a characteristic hysteresis loop related to a mesoporous solid. The BET surface areas of the supported NiAl precursors (54 m^2 g^{-1} for NiAl-CeO_2 and 52 m^2 g^{-1} for NiAl-CZ) were significantly higher compared to their bare supports (28 and 24 m^2 g^{-1}, respectively) which was assigned to the contribution of the high area of the spinel. Indeed, the BET surface area of the bulk NiAl was around 90 m^2 g^{-1}. It should be noted that after the reduction process the samples preserved their high surface areas (Table 1).

Table 1: Physico-chemical properties of the synthesised Ni-based catalysts.

Catalyst	Ni, wt.%	S_{BET}, m^2 g^{-1}	Ni^0_{TEM}, nm	D, %	S_{Ni}, m^2 g^{-1}	H_2 uptake of the support, mmol g^{-1}
NiAl-CeO_2	14	48	12	11	8	0.66
NiAl-CZ	14	48	8	15	10	0.25
NiAl	31	78	12	10	17	-

The reducibility of the samples was examined by means of temperature-programmed reduction with H_2 up to 950 ºC with a subsequent isothermal step for 0.5 h. The corresponding H_2-TPR profiles are plotted in Figure 1. The reduction curve of the bulk NiAl precursor displayed a broad feature at about 790 ºC, typical of the

reduction of the nickel aluminate phase (Boukha et al., 2016). Likewise, a small contribution was also observed at approximately 450 ºC related to the reduction of free NiO species not properly incorporated in the spinel lattice, which probably was not detected by XRD because of its crystallite size was very small and/or it was highly dispersed on the surface of the spinel. As the measured consumption of hydrogen coincided with the stoichiometric uptake necessary to reduce the nickel aluminate, it was proven that nickel was fully reduced. When analysing the reducibility of the supported NiAl catalysts it was found that the experimental hydrogen consumption was above the corresponding theoretical value required to reduce just the nickel present. Taking into account that that the reduction of the nickel aluminate was complete in the supported NiAl catalysts (as corroborated by XRD) it could be concluded that the ceria-based supports were also reduced during the process. Therefore, from the difference between the overall reducibility of the catalyst and the H_2 uptake linked to the nickel present the reducibility of the support was estimated for each sample (Table 1). Although the reduction of CZ present in the catalyst was complete (100 %) and CeO_2 was only partially reduced (60 %) it was clear that the overall H_2 uptake associated with the support was still considerably higher for NiAl-CeO_2 (0.66 mmol H_2 g^{-1}) with respect to NiAl-CZ (0.25 mmol H_2 g^{-1}). As for the shape of the reduction profiles of supported NiAl catalysts, these were very similar to the trace of bulk NiAl. After a suitable curve fitting, based on the criterion that the accumulative area coincided with the stoichiometric consumption of the nickel species with respect to the overall reduction of the catalysts, up to four H_2 uptakes could be distinguished; the features located at 350-450, 700 and 800 °C were assigned to the reduction of free nickel species, nickel not properly incorporated in the spinel lattice and nickel aluminate structure, respectively, while the remaining fourth peak was attributed to the reduction of the support.

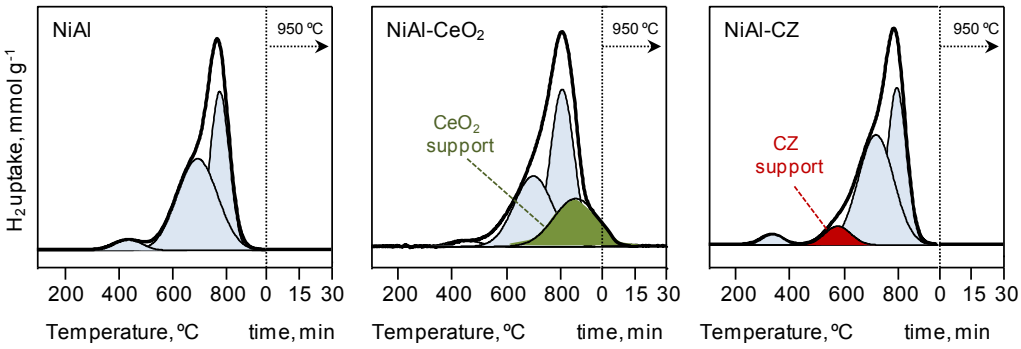

Figure 1: H_2-TPR profiles of a) bulk NiAl, b) NiAl-CeO_2 and c) NiAl-CZ.

Finally, the mean nickel particle size of the reduced catalysts was determined by TEM from the measurements of more than 250 particles. The obtained values were roughly similar for both NiAl-CeO_2 and NiAl-CZ catalysts, 12 nm and 8 nm, respectively and they were comparable to the mean size of the bulk NiAl spinel (12 nm) as well. From these data and following the procedure of Borodzinski and Bonarowska (1997), the dispersion percentage (D) and the accessible nickel surface (S_{Ni}) were calculated for each catalyst (Table 1). According to the reported results, both samples exhibited a similar available nickel surface, namely 10 m^2 g^{-1} for NiAl-CeO_2 and 8 m^2 g^{-1} for NiAl-CZ.

3.2 Catalytic performance in the SRM reaction

The catalytic behaviour of the catalysts was initially investigated for the methane steam reforming. Runs were carried out with a H_2O/CH_4 feed of 3 and at a VHSV of 38.4 L CH_4 g^{-1} h^{-1}. A light-off curve from 200 to 850 ºC was performed so as to analyse the effect of the temperature. As an example, the results corresponding to the NiAl-CZ catalyst are discussed. The observed activity was zero up to 700 ºC. However, at this temperature a very high conversion (90 %) was attained. With the aim of better understanding this atypical behaviour the sample used for reaction until 700 ºC was characterised. Thus, the XRD pattern revealed that at low temperatures the active phase (metallic nickel) was appreciably oxidised in the presence of water vapour with the consequent weakening of the nickel signal. Above this critical temperature, the reforming reaction was activated, leading to a sharp increase in hydrogen and CO yields, which rapidly reduced the nickel oxide to metallic nickel. For this reason, the catalytic test sequence was modified by starting from the highest temperature (850 ºC) and progressively decreasing down to 200 ºC. Under these changed operation conditions, a conversion profile without abrupt slope variations was obtained, indicating that the metal phase was maintained in its reduced state.

Figure 2 illustrates the evolution of the methane conversion, X_{CH4}, and hydrogen yield, Y_{H2}, with temperature and Table 2 summarises the activity data between 650-850 ºC. The following activity order was found: NiAl-CZ > Rh/Al_2O_3 > NiAl > NiAl-CeO_2. Thus, the spinel supported on the mixed oxide (NiAl-CZ) exhibited the best catalytic performance (close to that predicted by thermodynamics). For example, at 700 °C NiAl-CZ achieved a X_{CH4}= 93 % and Y_{H2}=1.73 against X_{CH4}=76 % and Y_{H2}=1.40 given by its counterpart supported on ceria (NiAl-CeO_2) while the reference catalysts, Rh/Al_2O_3 and NiAl, also showed lower values (X_{CH4}=82 %; Y_{H2}=1.52 and X_{CH4}=90 % and Y_{H2}=1.67, respectively). As for the supported catalysts (NiAl-CeO_2 and NiAl-CZ) the different behaviour was correlated to the composition of the support since the metallic surface area was comparable. In fact, the characterisation of the spent samples evidenced that the surface area decreased considerably for NiAl-CeO_2 catalyst (from 48 to 33 $m^2\ g^{-1}$) whereas the NiAl-CZ sample better preserved its high surface area (from 48 to 43 $m^2\ g^{-1}$). This observation suggested that the lesser performance of NiAl-CeO_2 could be justified by the low hydrothermal stability of ceria (Wang et al., 2015). The analysis of the ceria submitted to a thermal aging at 850 ºC under humid conditions (30 %H_2O/ 70 %N_2) indeed revealed a dramatic loss of surface area (from 30 to 4 $m^2\ g^{-1}$) and a lower overall reducibility (from 1.63 to 1.10 mmol $H_2\ g^{-1}$). Moreover, the oxidation of the metal phase to NiO was also observed in NiAl-CeO_2, whereas in the mixed oxide-based catalyst the active phase appeared to be stable (in other words, nickel oxides, such as, NiO or $NiAl_2O_4$ were no detected in its XRD pattern). Therefore, the nickel aluminate supported on ceria-zirconia (NiAl-CZ) resulted the best catalyst for the steam reforming of methane.

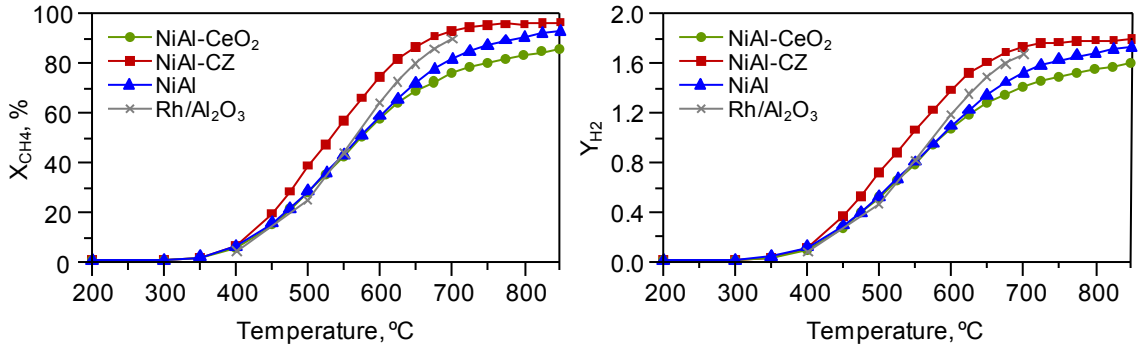

Figure 2: Evolution of methane conversion and yield of hydrogen as a function of temperature.

Table 2: Activity data of the investigated catalysts for SRM.

T, ºC	NiAl-CeO_2			NiAl-CZ			NiAl			Rh/Al_2O_3		
	$Y(H_2)$	H_2/CO	CO/CO_2	$Y(H_2)$	H_2/CO	CO/CO_2	$Y(H_2)$	H_2/CO	CO/CO_2	$Y(H_2)$	H_2/CO	CO/CO_2
650	1.28	8.7	0.7	1.61	7.5	1.0	1.34	9.4	0.7	1.48	7.5	1.0
700	1.41	7.5	1.0	1.73	6.6	1.3	1.52	7.7	0.9	1.67	6.8	1.2
750	1.49	6.7	1.3	1.77	6.1	1.6	1.63	6.7	1.3	-	-	-
800	1.55	6.3	1.5	1.78	5.8	1.8	1.68	6.2	1.5	-	-	-
850	1.60	5.9	1.7	1.79	5.5	2.1	1.73	5.8	1.8	-	-	-

Next, for this catalyst the influence of the water in the feedstream on the reaction was analysed. For this purpose, the reaction was carried out using different H_2O/CH_4 molar ratios (4, 3, 2 and 0.60) in the feed keeping constant the other operating parameters. The obtained results in methane conversion and hydrogen yield of hydrogen showed a clear trend: the higher the amount of water in the feed the better catalytic behaviour was achieved. However, this improvement was more evident up to the H_2O/CH_4=3 molar ratio; above this value there was no significant promotion. For instance, at 700 ºC the hydrogen yield varied from 1.02, 1.28, 1.61 and 1.73 for 0.6, 1, 2 and 3 H_2O/CH_4 molar ratios, respectively, but it only increased up to 1.77 for H_2O/CH_4 =4. On the other hand, it was visible that both methane conversion and hydrogen yield increased considerably with the temperature up to 700 ºC. Above this temperature, the values remained almost invariable. Further, it was observed that the yield of CO_2 notoriously increased up to 550 ºC as a result of the water gas shift reaction; however, at higher temperatures the presence of CO_2 decreased gradually because the reverse water gas shift reaction was favoured.

3.3 Catalytic performance in the POM reaction

In order to gain insight into the feasibility of the synthesised catalysts for other methane reforming technologies, their catalytic activity was also evaluated for partial oxidation of methane. In this case the reaction was studied at constant temperature (700 ºC) with the same VHSV (38.4 L CH_4 g^{-1} h^{-1}) and a stoichiometric O/C molar ratio (O/C=1) during a relatively short time interval (3 h). The activity data (Figure 3) revealed a notable performance for both supported NiAl catalysts. In fact, the two samples reached almost an identical conversion value as high as 72 %. Besides, no appreciable differences in product distribution were observed (Y_{H2}=0.67, H_2/CO=2.2 and CO/CO_2=4.6). On the basis of these comparable results, unlike SRM, it could be stated that the catalytic performance of the supported samples under POM stoichiometric conditions was only a function of the properties of the metallic phase and it was not controlled by other factors such as the overall reducibility. In other words, the activity was not dependent on the composition of the ceria-based support. On the other hand, it is recalled that no coke formation was observed. As for the reference reforming catalysts, the achieved activity over the bulk NiAl (X_{CH4}=77 %, Y_{H2}=0.72) was very similar despite the fact that the nickel loading was two times higher (31 wt.% vs. 14 wt.% of the supported catalysts). When compared to the noble metal-based catalyst (Rh/Al_2O_3) (X_{CH4}=82 %, Y_{H2}=0.79), the activity was slightly lower.

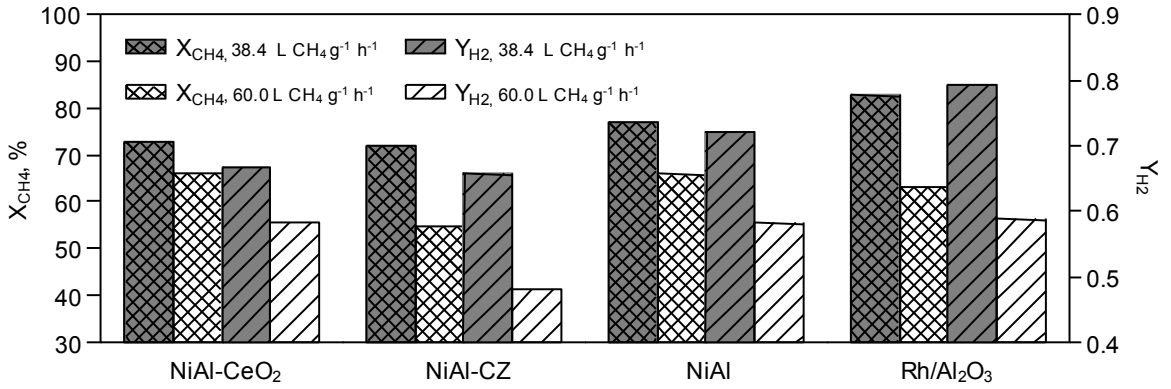

Figure 3: Performance of the investigated catalysts for *POM reaction under different operating conditions.*

With the aim of clarifying if the composition of the support would be a determining factor in optimising the behaviour of the final catalyst, POM reaction was investigated under more severe conditions, specifically, inducing an environment prone to coke formation. For this purpose, the O/C molar ratio was decreased from 1 to 0.8, the VHSV was increased up to 60 L CH_4 g^{-1} h^{-1} and the reaction time interval was prolonged up to 30 h. Figure 3 includes the methane conversion, yield of hydrogen, H_2/CO and CO/CO_2 molar ratio values corresponding to the end of the examined time interval. It should be noted that irrespective of the achieved conversion level all studied catalysts showed a marked stability. In this case, it was found that the supported NiAl catalysts behaved in a different way. The reported data clearly evidenced that NiAl-CeO_2 and the bulk NiAl sample were the most active catalysts, even reaching the conversion value predicted by thermodynamics (X_{CH4}=66 %, Y_{H2}=0.59-0.62). The performance of Rh-based catalyst was comparable (X_{CH4}=63 %, Y_{H2}=0.59). Conversely, the NiAl-CZ catalyst exhibited a worse activity in terms of both conversion and hydrogen production (X_{CH4}=55 %, Y_{H2}=0.48). In order to understand the causes for the different catalytic behaviour between NiAl-CeO_2 and NiAl-CZ, an exhaustive characterisation of the used samples was performed by XRD, N_2 physisorption, TGA-MS, TEM and Raman spectroscopy. The diffraction patterns revealed on one hand, the absence of NiO phase and, on the other hand, an important sintering on both catalysts. Surprisingly, the degree of this growth in the metallic particle size was larger for NiAl-CeO_2 (24 nm as determined by XRD) compared to NiAl-CZ (17 nm). Consequently, sintering did not appear to be responsible for the observed differences between both samples. In regard to coking, the presence of graphitic carbon was verified since the signal at 2θ=26.6° (JCPDS 89-8487) was undoubtedly visible. However, as the eventual formation of amorphous carbon could not be identified by XRD, the spent samples were also analysed by Raman spectroscopy. After curve fitting of the spectra using Lorentzian lines two main bands at 1360 and 1580 cm^{-1} along with a shoulder at 1610 cm^{-1} were distinguished. The signals at 1360 cm^{-1} (denoted as D band) and 1610 cm^{-1} (the so-called D' band) are associated with carbon with structural imperfections whereas the band at 1580 cm^{-1} (named as G band) is related to graphite layers (Pompeo et al., 2005). Taking the ratio of the areas of D and G bands (I_D/I_G) as an index for the crystalline order of the deposited filaments, it was found that both amorphous and graphitic filamentous carbon were present on the catalysts, with a similar distribution

(I_D/I_G=1.1). On the other hand, the specific surface area of the post-run samples considerably increased (from 48 $m^2\ g^{-1}$ for the freshly reduced samples to 74 $m^2\ g^{-1}$) due to the contribution of the porosity of the formed carbonaceous deposits. The total amount of coke deposited on the spent catalyst determined by TGA-MS was considerable and somewhat higher for the NiAl-CZ (55 wt.%) compared with that of NiAl-CeO_2 (49 wt.%). The combustion of coke occurred in both cases between 450-725 ºC and the oxidation profiles were characterised by a main peak at around 605 ºC and a shoulder approximately at 550 ºC. In the case of NiAl-CZ a small contribution of coke (10 %) was also distinguished at higher oxidation temperatures (685 ºC). According to the temperature range required for the complete combustion it could be assumed that nickel particles were mainly covered by filamentous carbon (Montero et al., 2014), which was further confirmed by TEM. Indeed, TEM images showed that these deposits were hollow carbon nanotubes with diameters in the 10-30 nm range and lengths around a micron.

In summary, based on the characterisation results it could be stated that slightly different amount of coke but with the same characteristics of morphology and crystalline order led to a somewhat different effect on the performance of the supported NiAl catalysts. In the case of NiAl-CeO_2 the conversion was hardly affected, which suggested that the high reducibility of its support was beneficial for maintaining the surface of the nickel particles free of carbonaceous deposits since it contributed to the gasification of this coke (Larimi and Alavi, 2012). In contrast, the NiAl-CZ catalyst exhibited a lower activity.

4. Conclusions

On the basis of the results presented in this work, nickel aluminate catalysts supported on ceria-based oxides appeared as a promising alternative to the reference Rh/Al_2O_3 catalyst for both steam reforming and partial oxidation of methane, due to their small metallic crystallites and high specific surface areas. In SRM, it was proved that the spinel supported on the mixed ceria-zirconia (NiAl-CZ) exhibited a better catalytic activity compared with its counterpart supported on pure ceria (NiAl-CeO_2) owing to its poor hydrothermal stability (marked loss of surface area and oxidation of the active metal phase). For POM carried out under mild reaction conditions (O/C=1; VHSV = 38.4 L $CH_4\ g^{-1}\ h^{-1}$), the used support had no influence on the catalytic behaviour since activity was noticeable and comparable over both catalysts. However, when more severe reforming conditions were employed, (O/C=0.8; VHSV = 60.0 L $CH_4\ g^{-1}\ h^{-1}$) the ceria-based catalyst was more efficient evidencing the beneficial effect of its higher reducibility that reduced the impact of carbonaceous deposits on the catalytic activity.

Acknowledgments

The authors wish to thank the financial support for this work provided by the Spanish Ministry of Economy and Competitiveness (ENE2013-41187-R) and the Basque Country Government (PRE_2015_2_0114).

References

Borodziński A., Bonarowska M., 1997, Relation between crystallite size and dispersion on supported metal catalysts, Langmuir, 13, 5613-5620.

Boukha Z., Jiménez-González C., Gil-Calvo M., de Rivas B., González-Velasco J.R., Gutiérrez-Ortiz J.I., López-Fonseca R., 2016, $MgO/NiAl_2O_4$ as a new formulation of reforming catalysts: Tuning the surface properties for the enhanced partial oxidation of methane, App. Catal. B: Environ., 199, 372-383.

Larimi A.S., Alavi S.M., 2012, Ceria-zirconia supported Ni catalysts for partial oxidation of methane to synthesis gas, Fuel, 102, 366-371.

Luisetto I., Tuti S., Battocchio C., Lo Mastro S., Sodo A., 2015, Ni/CeO_2-Al_2O_3 catalysts for the dry reforming of methane: The effect of $CeAlO_3$ content and nickel crystallite size on catalytic activity and coke resistance, Appl. Catal. A: Gen., 500, 12-22.

Montero C., Valle B., Bilbao J., Gayubo A.G., 2014, Analysis of Ni/La_2O_3-α-Al_2O_3 catalyst deactivation by coke deposition in the ethanol steam reforming, Chemical Engineering Transactions, 37, 481-486, DOI: 10.3303/CET1437081

Pompeo F., Nichio N.N., Ferretti O.A., Resasco D., 2005, Study of Ni catalysts on different supports to obtain synthesis gas, Int. J. Hydrogen Energy, 30, 1399-1405.

Roh H-S., Jun K-W., Dong W-S., Chang J-S., Park S-E., Joe Y-I., 2002, Highly active and stable Ni/Ce–ZrO_2 catalyst for H_2 production from methane, J. Mol. Catal. A: Chem., 181, 137-142.

Wang L., Huang M., Li B., Dong L., Jin G., Gao J., Ma J., Liu T., 2015, Enhanced hydrothermal stability and oxygen storage capacity of La^{3+} doped CeO_2-γ-Al_2O_3 intergrowth mixed oxides, Ceram. International, 41, 12988-12995.